Received: 5 March 2018 | Accepted: 10 May 2018

DOI: 10.1002/bio.3513

RESEARCH ARTICLE

WILEY LUMINESCENCE
The Journal of Biological and Chemical Luminescence

Enhanced photoluminescence properties of electrospun Dy^{3+}-doped ZnO nanofibres for white lighting devices

Chaitali Niranjan Pangul[1] | Shyamkant Wasudeorao Anwane[2] | Subhash Baburao Kondawar[1]

[1] Department of Physics, Rashtrasant Tukadoji Maharaj Nagpur University, Nagpur, India

[2] Department of Physics, Shivaji Science College, Nagpur, India

Correspondence
Subhash Baburao Kondawar, Department of Physics, Rashtrasant Tukadoji Maharaj Nagpur University, Nagpur, India.
Email: sbkondawar@yahoo.co.in

Funding information
Department of Science and Technology, India, Grant/Award Number: SR/FST/PSI-178/2012(C)

Abstract

Dy^{3+}-doped ZnO nanofibres with diameters from 200 to 500 nm were made using an electrospinning technique. The as-fabricated amorphous nanofibres resulted in good crystalline continuous nanofibres through calcination. Dy^{3+}-doped ZnO nanofibres were characterized using scanning electron microscopy (SEM), energy dispersive X-ray spectroscopy (EDX), X-ray diffraction (XRD), ultraviolet–visible (UV–vis) light spectroscopy, Fourier transform infrared spectroscopy (FTIR), and photoluminescence (PL). XRD showed the well defined peaks of ZnO. UV–vis spectra showed a good absorption band at 360 nm. FTIR spectra showed a Zn–O stretching vibration confirming the presence of ZnO. Photoluminescence spectra of Dy^{3+}-doped ZnO nanofibres showed an emission peak in the visible region that was free from any ZnO defect emission. Emissions at 480 nm and 575 nm in the Dy^{3+}-doped ZnO nanofibres were the characteristic peaks of dopant Dy^{3+} and implied efficient energy transfer from host to dopant. Luminescence intensity was found to be increased with increasing doping concentration and reduction in nanofibre diameter. Colour coordinates were calculated from photometric characterizations, which resembled the properties for warm white lighting devices.

KEYWORDS

Dy^{3+}-doped ZnO nanofibres, electrospinning, photoluminescence, white lighting devices

1 | INTRODUCTION

Semiconducting nanomaterials have found extensive interest amongst researchers due to their outstanding properties. Zinc oxide (ZnO) has been demonstrated to be one of the most versatile semiconductors, possessing excellent properties due its wide band gap energy (3.4 eV).[1] These astonishing properties have made ZnO a multifaceted candidate for various applications such as photocatalytic, optoelectronic, piezoelectric, luminescence devices and gas sensing methods.[2] Due to its outstanding optical properties, ZnO has become the most named semiconductor for use with a variety of dopants, especially for luminescence and rare earth ions. Efficient non-radiative electronic transition from the semiconductor host to the dopants has been the reason for the greatly enhanced luminescence of rare earth ions.[3] Intra-configurational $f-f$ transitions were the basis of photoluminescence spectroscopy of trivalent rare earth ions and gave their characteristic emission band.[4] Nd^{3+}- and Tm^{3+}-doped ZnO nanocrystals showed intense near-infrared emission lines with well resolved crystal-field (CF) splitting.[5] Zeng *et al.* have also observed the host-to-Eu^{3+} ET in ZnO:Eu^{3+} nanosheet-based hierarchical microspheres fabricated via a hydrothermal strategy.[6] Karthikeyan *et al.* investigated the spectroscopic properties of Dy^{3+} ion-doped zinc calcium tellurofluoroborate glass and observed white light emission in the glass.[7] Trivalent dysprosium ions exhibited important luminescence of two primary colour phosphors.[8] Dy^{3+} ion visible luminescence consisted of a yellow band at 570–600 nm corresponding to the $^4F_{9/2} \rightarrow {}^6H_{13/2}$ hypersensitive transition and a blue band at 470–500 nm corresponding to the $^4F_{9/2} \rightarrow {}^6H_{15/2}$ transition.[9] Additionally, Dy^{3+} ion emission strongly depended on the type of host matrix. Liu *et al.* synthesized Dy^{3+}-doped

Abbreviations used: CF, crystal-field; CIE, Commission Internationale de l'Eclairage; CRI, colour rendering index; DST, Department of Science and Technology; EDX, energy dispersive X-ray; FTIR, Fourier transform infra-red; LED, light-emitting diode; LER, luminescence efficacy of radiation; PL, photoluminescence; PVA, polyvinyl alcohol; SEM, scanning electron microscopy; UV, ultraviolet; XRD, X-ray diffraction.

 © 2018 John Wiley & Sons, Ltd.

ZnO nanocrystals that emitted intense and typical emission lines originating from the f–f transitions of Sm^{3+} and Dy^{3+} ions.[3]

Despite the amazing properties shown by existing nanomaterials, the pursuit of novel properties through new varieties of nanomaterials has always been of interest. For example, 0-D, 1-D, 2-D are diverse types of nanomaterials that behave differently due to their high surface area to volume ratio. Amongst these, 1-D nanomaterials such as nanowires, nanorods, nanotubes, nanobelts, nanofibres and nanoribbons have been studied increasingly due to their importance in research and development and have a wide range of potential applications due to their high aspect ratio. It is generally accepted that 1-D nanomaterials are ideal systems for exploring many novel phenomena at the nanoscale level and for investigating the size and dimensionality dependence of functional properties.[10] Yadav *et al*. synthesized Eu^{3+}-doped ZnO nanowires using a co-precipitation method and observed transition in the visible regions due to Eu^{3+} ions.[11] Ruqia *et al*. fabricated ZnO nanorods and studied their photoluminescence spectra, which showed intense UV emission.[12] Several methods for the synthesis of 1-D nanomaterials have been described, but electrospinning had proved to be the most effective way of generating nanofibres with fibre diameters in the range of a few tens to several hundred nanometres.[13] Liu *et al*. studied the effect of Ce doping on the optoelectronic and sensing properties of electrospun ZnO nanofibres and found that the photoluminescence integrated intensity ratio of UV emission to deep-level green emission for Ce-doped ZnO nanofibres was over twice than that of pure ZnO.[14] Zhang *et al*. found room temperature enhanced red emission from novel Eu^{3+}-doped ZnO nanocrystals uniformly dispersed in nanofibres.[15] Jong-Seong Bae and co-workers studied the preparation and characterization of Ce-doped ZnO nanofibres using an electrospinning method.[16]

Despite all the tremendous work taking place on the luminescence properties of ZnO 1-D nanomaterials there is still scope to investigate the effect of different dopants on ZnO to achieve more intense defect-free visible emissions. Within various applications of such advanced materials, luminescence from 1-D nanomaterials such as nanofibres provides flexibility for 'smart fabrics'. Luminescence from nanofibres could provide smart, flexible, lightweight and high definition textiles.[17] In the present study, we reported the construction of highly luminescent Dy^{3+}-doped ZnO nanofibres using an electrospinning method and its application for smart clothing and flexible light-emitting devices. The synthesized nanofibres underwent a calcination process to form inorganic nanofibres comprising nanocrystals of Dy^{3+}-doped ZnO nanofibres. These calcined nanofibres were examined using SEM, XRD, EDX, UV–vis absorbance spectroscopy and FTIR strategies. Photoluminescence studies were carried out to study the effect of Dy^{3+} ion doping into host ZnO and revealed effective energy transfer from host to dopant, resulting in enhanced luminescence from Dy^{3+} ions.

2 | EXPERIMENTAL

Zinc acetate (Zn $(CH_3COO)_2.H_2O$) from LobaChemie with 99.5% purity, dysprosium (III) nitrate (Dy $(NO_3)_3$) from Sigma Aldrich with 99.9% purity and polyvinyl alcohol (PVA) from Sigma Aldrich molecular weight: 89 000, were used as starting materials. All chemicals were used without any further purification. In the experimental procedure, 0.5 g of Zn $(CH_3COO)_2..H_2O$ and x% of (Dy $(NO_3)_3$) (x = 0, 1, 2) was first dissolved in deionised water. Another solution was prepared by dissolving 0.35 g of PVA in deionised water at 60 °C for 2 h. Zn $(CH_3COO)_2..H_2O$ and Dy $(NO_3)_3$ solution were added to the PVA solution slowly with acetic acid 0.059 g and the resultant solution was vigorously stirred for another 2 h to obtain an homogenous solution. The resultant solution was put in a syringe and the electrospinning experiment was then carried out. The distance between the syringe needle tip and collector aluminium foil was maintained at 15 cm and the high voltage 18 kV was applied. The ejection rate of aqueous solution from the syringe was maintained at 0.4 ml/h. The fibres were collected on grounded aluminium foil. The collection of as-spun fibres was dried in air at 120 °C for 12 h. Calcination was carried for the dried fibres at 300 °C for 2 h in order to form inorganic fibres.

The structure, morphology and size of the prepared samples were studied using an X-ray diffractometer (XRD) with a Cu Kα target (λ = 1.5418 Å) Rigaku, Miniflex 600. Scanning electron microscopy was performed on a Carl Zeiss EVO 18 SEM equipped with energy dispersive X-rays. UV–vis spectroscopy was carried out on a Carry 5000 spectrophotometer with full slit width and double beam mode. FTIR transmission spectroscopy was monitored on a Thermo Nicolet, Avatar 370 instrument. Photoluminescence measurements were

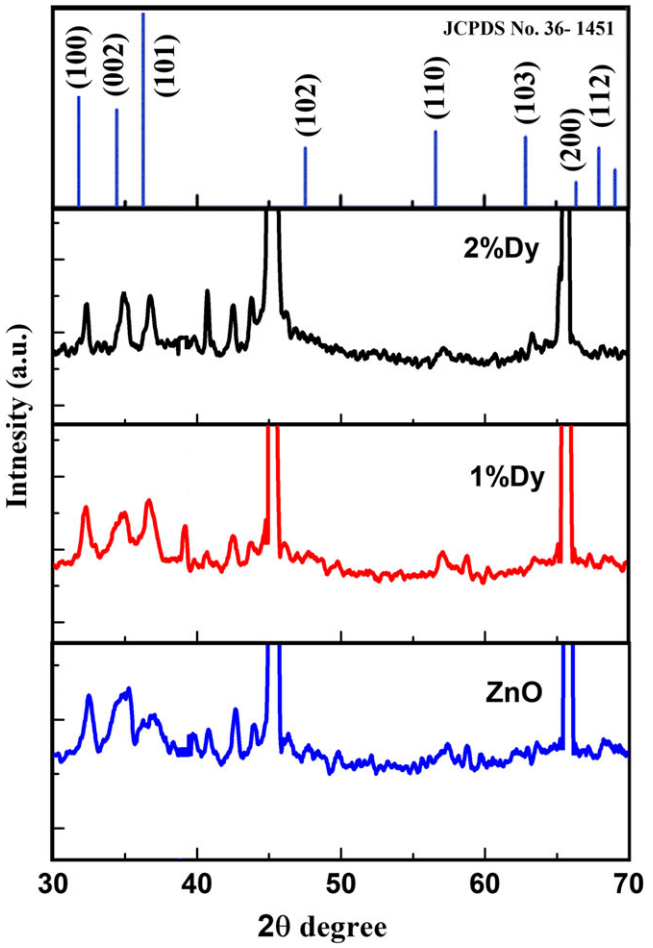

FIGURE 1 XRD patterns of calcined x% Dy^{3+}-doped ZnO nanofibres (x = 0, 1, 2)

performed using a Shimadzu RF-5301PC spectrophotometer at room temperature.

3 | RESULTS AND DISCUSSION

The x% Dy^{3+}-doped ZnO nanofibres (x = 0, 1, 2) were essentially amorphous in the as-synthesized form. Calcination at 300 °C resulted in well defined crystalline features. Figure 1 shows the XRD patterns of the prepared Dy^{3+}-doped ZnO nanofibres calcined at 300 °C for 2 h. All the samples clearly exhibited diffraction peaks that were the prominent peaks of the hexagonal wurtzite-type structure of zinc oxide (ZnO) (JCPDS No. 36–1451). No other peaks related to the Dy_2O_3 or Zn $(OH)_2$ were seen and confirmed that Dy^{3+} were successfully incorporated into ZnO.

Figure 2 shows the SEM images of x% Dy^{3+}-doped ZnO nanofibres (x = 0, 1, 2) calcined at 300°C. *SEM* images revealed ultralong, continuous, smooth, uniform naonofibres with random orientations fabricated by electrospinning. From the frequency distribution of pure ZnO nanofibres, Figure 2(a) shows that the average diameter of fibres was 270 nm. From the frequency distribution of 1% Dy-doped ZnO nanofibres, Figure 2(b) shows that the average diameter of fibres was 680 nm. From the frequency distribution of 2% Dy-doped ZnO nanofibres, Figure 2(c) shows that the average diameter of fibres was 420 nm. Even when PVA was removed by calcination, the prepared samples remained as continuous inorganic fibres. Figure 3 shows the EDX of the ZnO and Dy^{3+}-doped ZnO nanofibres calcined at 300 °C and confirmed the presence of elements Zn, O and Dy in the fabricated nanofibres.

Figure 4(a) shows the UV–vis absorption spectra of pure ZnO and Dy^{3+}-doped ZnO nanofibres calcined at 300°C. The absorption spectra of all the samples showed strong absorption at 360 nm which showed a blue shift compared with bulk ZnO.[18] This blue shift was explained by the quantum confinement effect as reduction of the particle size resulted in incredible potential properties.[19] Optical band

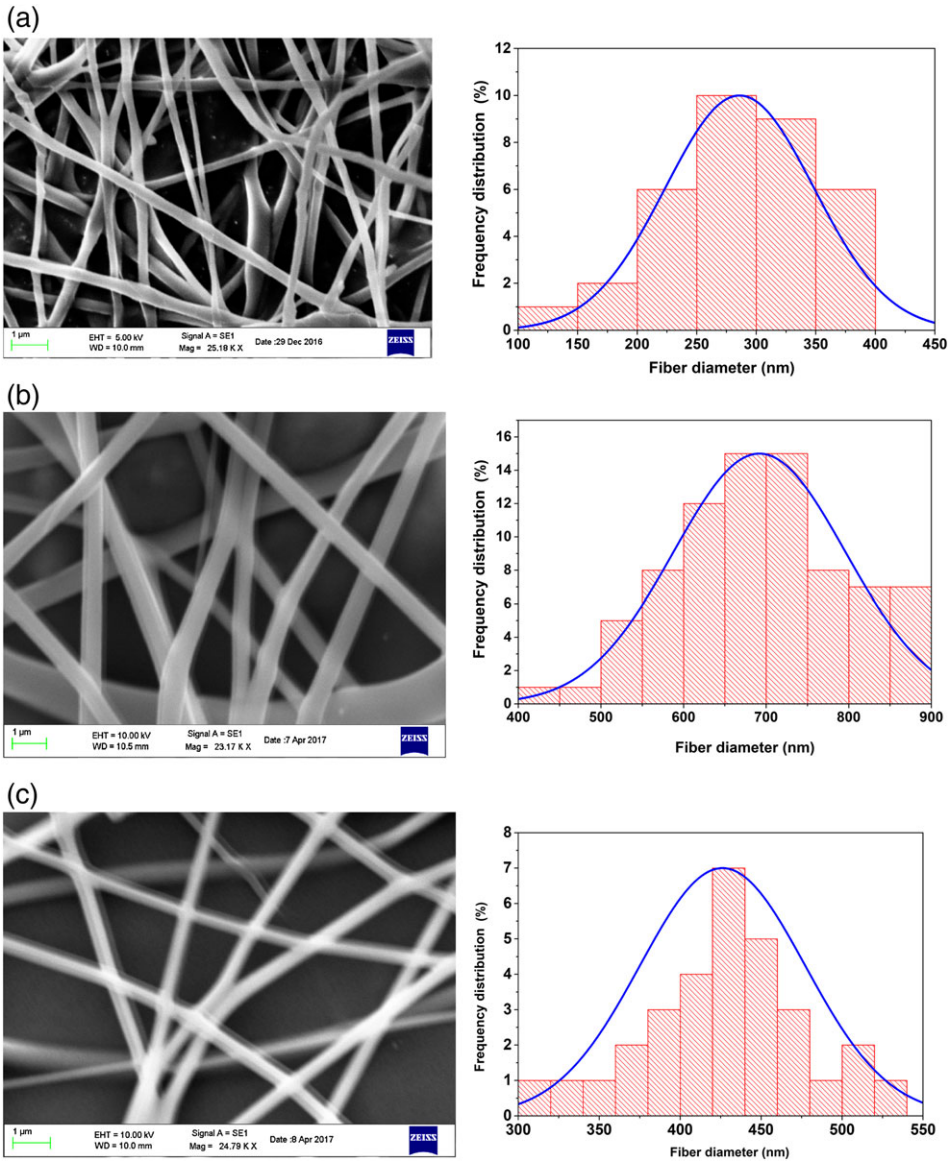

FIGURE 2 (a) SEM image of ZnO nanofibres calcined at 300°C. (b) SEM image of 1% Dy^{3+}-doped ZnO nanofibres calcined at 300°C. (c) SEM image of 2% Dy^{3+}-doped ZnO nanofibres calcined at 300°C

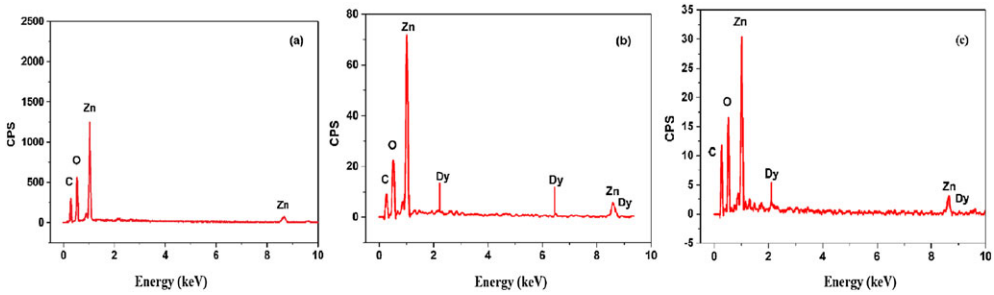

FIGURE 3 EDX spetra of calcined x% Dy^{3+}-doped ZnO nanofibres (x = 0, 1, 2)

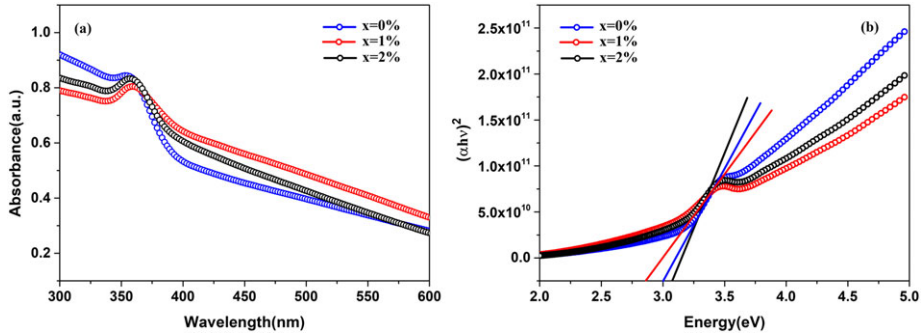

FIGURE 4 UV–vis absorption spectra and Tauc's plot of $(\alpha h\nu)^2$ versus h vof x% Dy^{3+}-doped ZnO nanofibre (x = 0, 1, 2) calcined at 300°C

gap was calculated using Tauc's plot. The frequency dependent absorption coefficient is given by

$$(\alpha h\nu)^{1/n} = A(h\nu - E)$$

where, α is the absorption coefficient calculated using the Beer–Lambert's relationship α=2.303 A/d, where A and d are the absorbance and the thickness of the film respectively, *h*vis the incident photon energy, while E is the optical band gap and *n* is the index showing the transitions in the semiconductors *n* = 1/2, 3/2, 2 and 3 for direct allowed, direct forbidden, indirect allowed and indirect forbidden transitions, respectively.[20,21] The graph between $(\alpha\ h\nu)^2$ (*n* = 1/2 is considered as ZnO is a direct band gap semiconductor) and *h* vgives the Tauc's plot and extrapolating $(h\nu)^2$ = 0 gives the value of the optical band gap of the semiconductor.[22–24] Figure 4(b) shows Tauc's plot between $(\alpha\ h\nu)^2$ and *h*vfor pure ZnO and Dy^{3+}-doped ZnO nanofibres calcined at 300°C. The optical band gap was found to vary with the doping concentration from 2.95 eV to 3.115 eV as well as with the decreasing diameter of the nanofibres. Band gap energy was found to be least for the fibres with a high diameter and showed the size-dependent properties of the band gap for the synthesized fibres.

Figure 5 shows the FTIR spectra of the pure ZnO and Dy^{3+}-doped ZnO nanofibres calcined at 300°C and PVA nanofibres. The characteristics peaks of PVA nanofibres at 1633.80, 1434.69, 1101.87, 841.32 cm^{-1} were assigned to the characteristic vibration bands of PVA. The band at 1633.80 cm^{-1} represents the carbonyl group, which is due to the absorption of the residual acetate group during PVA manufacture. The band around 1434.69 cm^{-1} was attributed to $-CH_3$ bending, while 1101.87 cm^{-1} is due to the v (C–O) stretching vibration, and the band at 841.32 cm^{-1} was assigned to the v (C–C)

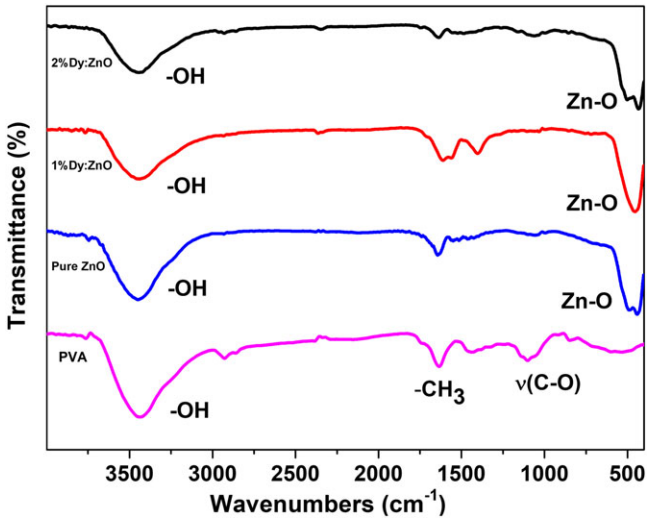

FIGURE 5 FTIR spectra of PVA nanofibres and calcined x% Dy^{3+}-doped ZnO nanofibres (x = 0, 1, 2)

stretching vibration. A very broad band around 3500 cm^{-1} was seen in all samples, and represented the –OH group and might be due to adsorption of ambient moisture. A strong band at 455.07 cm^{-1} of pure ZnO and Dy^{3+}-doped ZnO nanofibres was ascribed to the stretching vibration of metal bond (Zn–O) along with a peak at 501.11 cm^{-1}, which was associated with oxygen deficiency and/or defect complexes in ZnO.[25–27]

Figure 6 is the photoluminescence excitation and emission spectra of pure ZnO nanofibres calcined at 300°C. As seen in the figure, when excited at wavelength 343 nm two emission peaks were observed in the emission spectra. A narrow UV band related to near

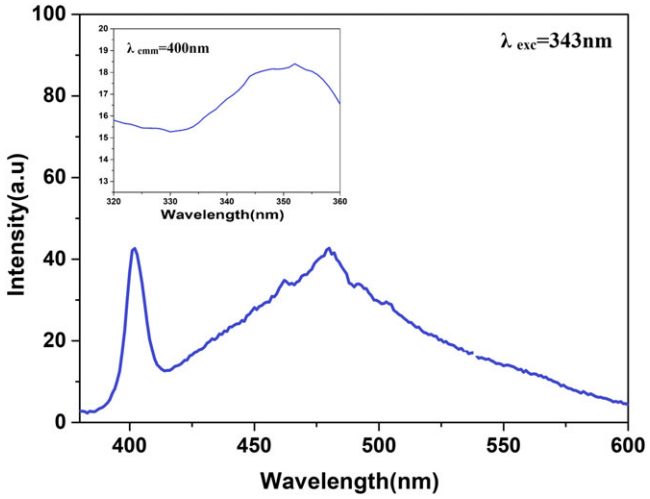

FIGURE 6 Photoluminiscence emission spectrum calcined pure ZnO nanofibres (inset: excitation spectrum)

band edge emission was observed at 400 nm along with the broad defect-related emission in the green region. The UV emission was assigned to free and bound exciton recombination, while the green emission was assigned to the oxygen vacancies. The excitation spectrum was monitored at wavelength 400 nm and a broad spectrum around 360 nm was observed, which could be accredited to the near band absorptions.[28,29]

Figure 7 is the photoluminescence excitation and emission spectra of x% Dy^{3+} ion-doped ZnO nanofibres (x = 1, 2). When excited at the excitation wavelength 353 nm two spectral peaks at 480 nm and 575 nm were observed in both of the prepared Dy^{3+} ion-doped ZnO nanofibres and represented the distinctive emission peak of Dy^{3+} ions, $^4F_{9/2} \rightarrow {}^6H_{15/2}$ and $^4F_{9/2} \rightarrow {}^6H_{13/2}$ respectively. With respect to dysprosium, the $^4F_{9/2} \rightarrow {}^6H_{15/2}$ transition is a magnetically allowed transition while $^4F_{9/2} \rightarrow {}^6H_{13/2}$ is a forced electrical transition.[30,31] The asymmetry ratio $^4F_{9/2} \rightarrow {}^6H_{13/2}/{}^4F_{9/2} \rightarrow {}^6H_{15/2}$ is the measure of site symmetry in which dysprosium is situated. The $^4F_{9/2} \rightarrow {}^6H_{13/2}$ transition was allowed only when Dy^{3+} ions were located at low symmetries with no inversion centre, whereas when situated at high symmetries with an inversion centre the transition $^4F_{9/2} \rightarrow {}^6H_{15/2}$ was prominent.[32] The Y/B ratio was calculated for the dataset and found to decrease with increasing doping concentration from 3.58 to 2.93. With incorporation of Dy^{3+} into ZnO the NBE and DLE of ZnO were overtaken by the characteristic emission of Dy^{3+} ions.[33,34] No emission related to UV transition or ZnO defects was observed and implied the effective energy transfer from host ZnO to the dopant Dy^{3+} ions. Such defect-free visible emission from ZnO enabled the prepared material to be an interesting candidate for flexible light-emitting diodes (LEDs). An energy transfer diagram is illustrated in Figure 8. Upon excitation the host excited to the Conduction Band, an effective transfer from dopant host took place that then excited the dopant ion Dy^{3+} from ground state to the $^6P_{7/2}$ excited state. This excited ion underwent non-radiative relaxation to reach the $^4F_{9/2}$ level. While approaching the background state the dopant ion radiated energy in the form of light and corresponding to various ground state levels. The excitation spectrum was monitored at dominant 575 nm and a broad spectrum around 350 nm was observed that again contributed to the excitation of host ZnO.[35,36] It was clearly seen that the intensity increased with increasing concentration of dysprosium from 1% to 2%.

The Commission Internationale de l'Eclairage (CIE) parameters such as colour coordinates, colour co-related temperature (CCT),

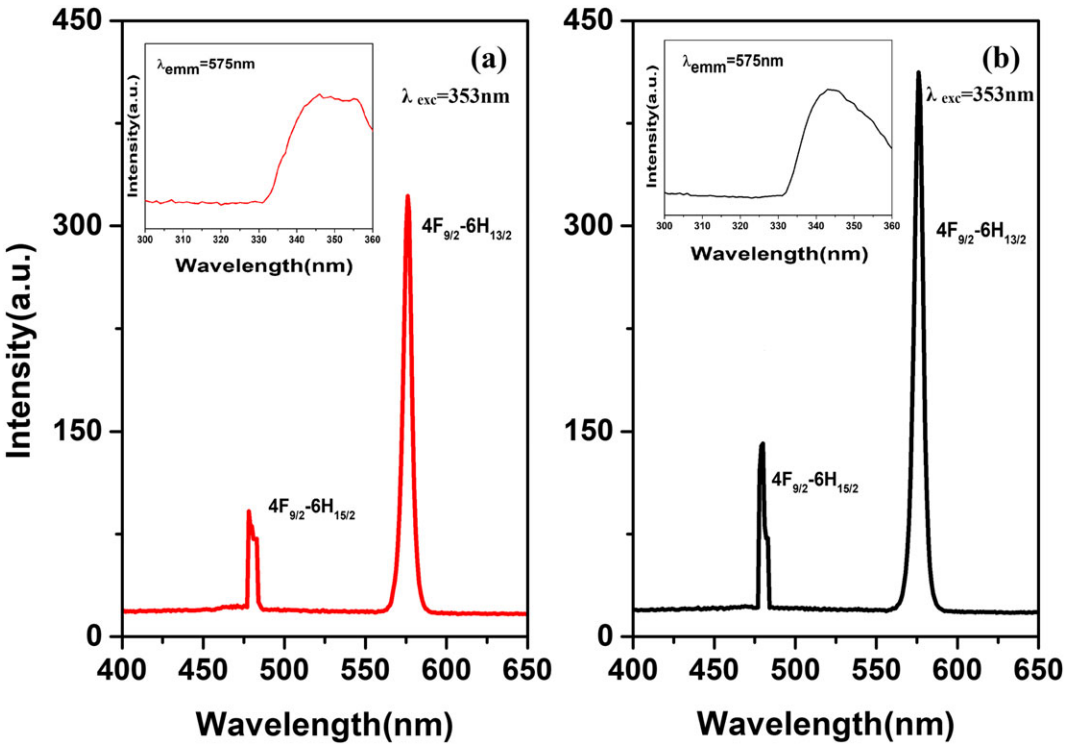

FIGURE 7 Photoluminiscence emission spectra of calcined (a) 1% Dy^{3+}-doped ZnO nanofibres and (b) 2% Dy^{3+}-doped ZnO nanofibres [inset: excitation spectra for (a) 1% and (b) 2% Dy^{3+}-doped ZnO nanofibres]

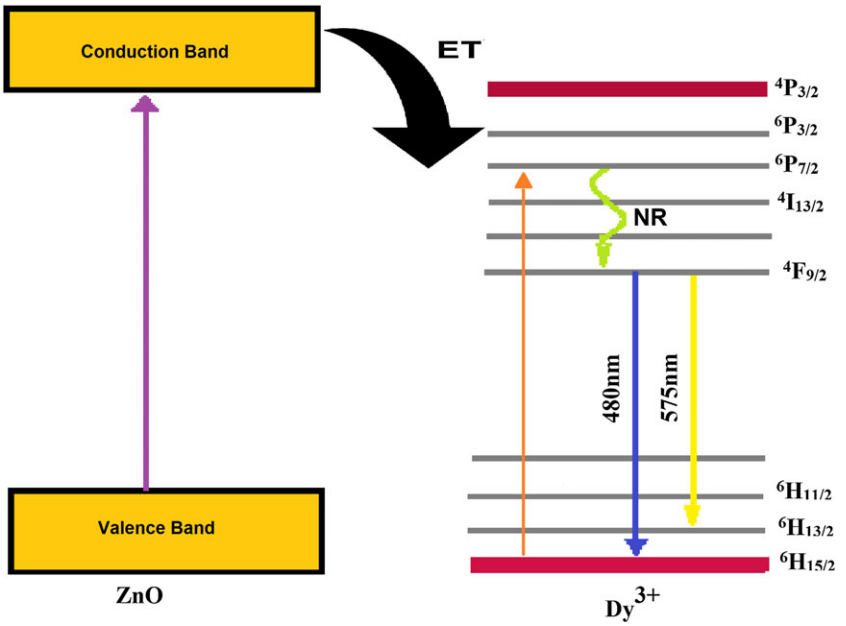

FIGURE 8 Energy transfer diagram of ZnO and Dy^{3+} ions

luminescence efficacy of radiation (LER) and colour rendering index (CRI) were calculated to give the photometric characteristics of the prepared nanofibres. Figure 9 illustrates the CIE chromaticity diagram of emission spectra of the prepared samples. The parameters were calculated by a spectrophotometric method using the spectral energy distribution of the chromaticity diagram and are summarized in Table 1.

The colour coordinates (x, y) were calculated using the standard procedure.[37] Colour coordinates are one of the important parameters for evaluating luminescent material performance. From the chromaticity diagram, it was seen that the coordinates transversed from the blue region to the white region with doping of dysprosium into ZnO. Thus, colour tunability could be achieved by changing the doping concentration. It is evident from the obtained CCT, CRI and LER values as given in Table 1, that Dy^{3+} ion-doped ZnO nanofibres calcined at 300°C seem to be good candidates for warm white light LED devices.[38–40]

TABLE 1 Photometric characteristics of prepared nanofibres

Samples	CIE x	CIE y	CCT	CRI	LER (lm/W)
ZnO nanofibres	0.2656	0.2964	11205	93	240
1% Dy ZnO nanofibres	0.3779	0.3925	4175	38	315
2% Dy ZnO nanofibres	0.3784	0.3981	4195	33	324

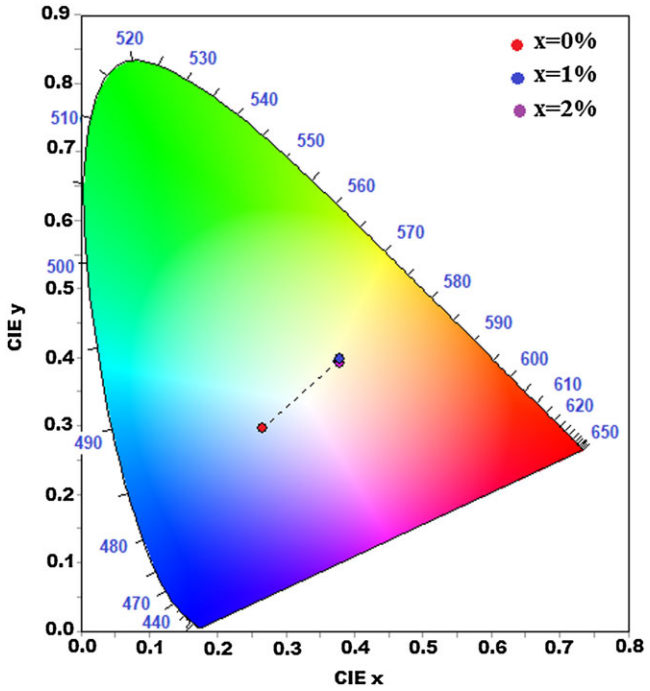

FIGURE 9 CIE diagram of emission spectra of x% Dy^{3+}-doped ZnO nanofibres (x = 0, 1, 2)

4 | CONCLUSION

Dy^{3+}-doped ZnO nanofibres with diameters in the range 200 to 500 nm were made successfully by electrospinning. Photoluminescence revealed that the electrospun Dy^{3+}-doped ZnO nanofibres possessed more intense emission in the visible and were region free from ZnO defects, resulting from effective energy transfer from host ZnO to dopant Dy^{3+}. Enhanced visible light luminescence transverse from the blue region to the white region was observed in the CIE diagram with increasing doping concentrations. The as-fabricated Dy^{3+}-doped ZnO nanofibres could be used in various applications such as flexible light emitting displays, banners, smart clothing, etc.

ACKNOWLEDGEMENTS

This work was supported by the Department of Science and Technology (DST, New Delhi, India) Support under DST-FIST Program, Grant No. SR/FST/PSI-178/2012(C).

ORCID

Subhash Baburao Kondawar http://orcid.org/0000-0002-7465-706X

REFERENCES

[1] Y. Park, C. Litton, T. Collins, D. Reynolds, *Physiol. Rev.* **1966**, *143*, 512.

[2] M. Samadi, M. Zirak, A. Naseri, E. Khorashadizade, A. Z. Moshfegh, *Thin Solid Films* **2016**, *605*, 2.

[3] Y. Liu, R. Li, W. Luo, H. Zhu, X. Chen, *Spect. Lett.* **2010**, *43*, 343.

[4] J. C. G. Bunzli, Luminescent Probes, Lanthenides Probes in Life, Chemical and Earth Sciences, Theory and Practice, Ch. 7, **1989**, 219.

[5] Y. Liu, W. Luo, R. Li, H. Zhu, X. Chen, *Opt. Exps.* **2009**, *17*, 9748.

[6] X. Zeng, J. Yuan, Z. Wang, L. Zhang, *Adv. Mater.* **2007**, *19*, 4510.

[7] P. Karthikeyan, S. Arunkumar, K. Annapoorani, K. Marimuthu, *Spectrochim. Acta A* **2018**, *0193*, 422.

[8] J. Pisarska, *Opt. Mater.* **2009**, *31*, 1784.

[9] F. Gu, S. Wang, M. Lu, G. Zhou, D. Xu, D. Yuan, *Langmuir* **2004**, *20*, 3528.

[10] J. Tiwari, R. Tiwari, K. Kim, *Prog. Mater. Sci.* **2012**, *57*, 724.

[11] R. Yadav, A. Pandey, S. S. Sanjay, *Chalcogenide Lett.* **2009**, *6*, 233.

[12] B. Ruqia, K. Nam, H. Lee, G. Lee, S. Choi, *Cryst. Eng. Comm.* **2017**, *19*, 1454.

[13] N. Tucker, J. Stanger, M. Staiger, H. Razzaq, K. Hofman, *J. Engg. Fib. Fab. Sp. Issue* **2012**, *7*, 63.

[14] Y. Liu, H. Zhang, X. Yan, A. Zhao, Z. Zhang, W. Si, M. Gong, J. Zhang, Y. Long, *RSC Adv.* **2016**, *6*, 85727.

[15] Y. Zhang, Y. Liu, X. Li, Q. Wang, E. Xie, *Nano. Tech.* **2011**, *22*. 415702

[16] J. Bae, M. Won, J. Yoon, B. Lee, E. Pak, H. Seo, J. Kim, *J. Analy. Sci. Tech.* **2011**, *2*, 1.

[17] X. Tao, *Smart Fibres*, Fabrics and Clothing, CRC Press LLC **2000**.

[18] A. Roy, S. Gupta, S. Sindhu, A. Parveen, P. Ramamurthy, *Composites B* **2013**, *47*, 314.

[19] U. Manzoor, M. Islam, L. Tabassam, S. Rahman, *Phys. E* **2009**, *41*, 1669.

[20] P. Sahay, R. Nath, S. Tewari, *Cryst. Res. Technol.* **2007**, *42*, 275.

[21] A. Mansour, S. Mansour, M. Abdo, *J. Appl. Phys.* **2015**, *7*, 60.

[22] B. Lokhande, M. Uplane, *Appl. Surf. Sci.* **2000**, *167*, 243.

[23] A. Zaouia, M. Zaouia, S. Kacimia, A. Boukorttb, B. Bouhafsa, *Mater. Chem. Phys.* **2010**, *120*, 98.

[24] B. Lokhande, P. Patil, M. Uplane, *Phys. B* **2001**, *59*, 302.

[25] S. Rajendran, M. Sivakumar, R. Subadevi, *Sol. Stat. Ionics* **2004**, *167*, 335.

[26] A. Akhavan, F. Khoylou, E. Ataeivarjov, *Rad. Phy. Chem.* **2017**, *138*, 49.

[27] E. Ghafari, Y. Feng, Y. Liu, I. Ferguson, N. Lu, *Composites B* **2017**, *116*, 40.

[28] E. Tomzig, R. Helbig, *JOL* **1976**, *14*, 403.

[29] K. Vanheusden, C. Seager, W. Warren, D. Tallant, J. Caruso, M. Hampden-Smith, T. Kodas, *JOL* **1997**, *75*, 11.

[30] R. Sreedharan, R. Krishnan, G. Kumar, V. Kavitha, S. Chalana, R. Bose, S. Suresh, R. Vinodkumar, S. Sudheer, V. M. Pillai, *J. Alloys Compd.* **2017**, *721*, 661.

[31] G. Amira, B. Chaker, E. Habib, *Spectrochim. Acta A* **2017**, *177*, 164.

[32] C. Manjunatha, D. Sunitha, H. Nagabhushana, B. Nagabhushana, S. Sharma, R. P. S. Chakradhar, *Spectrochim. Acta A* **2012**, *93*, 140.

[33] N. Narayanan, N. Deepak, *Optik* **2018**, *158*, 1313.

[34] F. Pavón, A. Urbieta, P. Fernández, *JOL* **2018**, *195*, 396.

[35] Z. Hou, R. Chai, M. Zhang, C. Zhang, P. Chong, Z. Xu, *Langmuir* **2009**, *25*, 12340.

[36] V. Hingwea, K. Koparkara, N. Bajajb, S. Omanwara, *Optik* **2017**, *140*, 211.

[37] S. G. Itankar, M. P. Dandekar, S. B. Kondawar, B. M. Bahirwar, *Luminescence* **2017**, *32*, 1535.

[38] M. Janulevicius, P. Marmokas, M. Misevicius, J. Grigorjevaite, L. Mikoliunaite, S. Sakirzanovas, A. Katelnikovas, *Sci. Rep.* **2016**, *6*, 26098.

[39] A. Ambast, J. Goutam, S. Som, S. Sharma, *Spectrochim. Acta A* **2014**, *122*, 93.

[40] P. Haritha, I. Martín, C. Viswanath, N. Vijaya, K. Krishnaiah, C. Jayasankar, D. Haranath, V. Lavín, V. Venkatramu, *Opt. Mater.* **2017**, *70*, 16.

How to cite this article: Pangul CN, Anwane SW, Kondawar SB. Enhanced photoluminescence properties of electrospun Dy^{3+}-doped ZnO nanofibres for white lighting devices. *Luminescence*. 2018;1–7. https://doi.org/10.1002/bio.3513